Dossier

This paper is a part of the hereunder thematic dossier published in OGST Journal, Vol. 70, No. 1, pp. 3-211 and available online here

Cet article fait partie du dossier thématique ci-dessous publié dans la revue OGST, Vol. 70, n°1, pp. 3-211 et téléchargeable ici

DOSSIER Edited by/Sous la direction de : **B. Leduc et P. Tona**

IFP Energies nouvelles International Conference / Les Rencontres Scientifiques d'IFP Energies nouvelles
E-COSM'12 — IFAC Workshop on Engine and Powertrain Control, Simulation and Modeling
E-COSM'12 — Séminaire de l'IFAC sur le contrôle, la simulation et la modélisation des moteurs et groupes moto-propulseurs

Oil & Gas Science and Technology – Rev. IFP Energies nouvelles, Vol. 70 (2015), No. 1, pp. 3-211

IFP Energies nouvelles

Oil & Gas Science and Technology – Rev. IFP Energies nouvelles, Vol. 70 (2015), No. 1, pp. 179-194

DOI: 10.2516/ogst/2013207

IFP Energies nouvelles International Conference
Rencontres Scientifiques d'IFP Energies nouvelles

E-COSM'12 - IFAC Workshop on Engine and Powertrain Control, Simulation and Modeling
E-COSM'12 - Séminaire de l'IFAC sur le contrôle, la simulation et la modélisation des moteurs et groupes moto-propulseurs

Design Methodology of Camshaft Driven Charge Valves for Pneumatic Engine Starts

Michael M. Moser*, Christoph Voser, Christopher H. Onder and Lino Guzzella

Institute for Dynamic Systems and Control, ETH Zurich, Sonneggstrasse 3, 8092 Zurich - Switzerland
e-mail: mimoser@ethz.ch - voserc@ethz.ch - onder@ethz.ch - lguzzella@ethz.ch

* Corresponding author

Abstract — *Idling losses constitute a significant amount of the fuel consumption of internal combustion engines. Therefore, shutting down the engine during idling phases can improve its overall efficiency. For driver acceptance a fast restart of the engine must be guaranteed. A fast engine start can be performed using a powerful electric starter and an appropriate battery which are found in hybrid electric vehicles, for example. However, these devices involve additional cost and weight. An alternative method is to use a tank with pressurized air that can be injected directly into the cylinders to start the engine pneumatically. In this paper, pneumatic engine starts using camshaft driven charge valves are discussed. A general methodology for an air-optimal charge valve design is presented which can deal with various requirements. The proposed design methodology is based on a process model representing pneumatic engine operation. A design example for a two-cylinder engine is shown, and the resulting optimized pneumatic start is experimentally verified on a test bench engine. The engine's idling speed of 1200 rpm can be reached within 350 ms for an initial pressure in the air tank of 10 bar. A detailed system analysis highlights the characteristics of the optimal design found.*

Résumé — **Méthodologie pour le design des valves de chargement opérées par arbre à cames** — Les pertes à vide représentent une partie essentielle de la consommation des moteurs à combustion interne. La mise à l'arrêt du moteur pendant la marche à vide peut, par conséquent, en améliorer son efficacité générale. Pour être accepté par le conducteur, le redémarrage du moteur doit être rapide. On peut réaliser ce démarrage rapide du moteur, moyennant un démarreur électrique puissant conjointement avec un accumulateur approprié, solution retenue par exemple, pour les véhicules à système hybride électrique. Cependant, ces derniers augmentent le coût et le poids. Une alternative consiste dans le démarrage pneumatique du moteur en utilisant de l'air comprimé stocké dans un réservoir sous pression et injecté directement dans les cylindres. Cette étude présente le démarrage pneumatique du moteur en utilisant des valves de chargement commandées par arbre à cames. On présente une méthodologie visant à une consommation de l'air optimale en mesure de respecter des exigences différentes. La démarche proposée s'appuie sur le modèle d'un processus représentant l'opération pneumatique du moteur. La vérification expérimentale du démarrage pneumatique est réalisée et optimisée sur un moteur 2 cylindres sur banc d'essai. Avec une pression initiale de 10 bar dans le reservoir d'air, la vitesse de rotation à vide de 1 200 tr/min peut être atteinte en 350 ms. Une analyse détaillée confirme les caractéristiques du système optimisé.

INTRODUCTION

An inherent property of Internal Combustion Engines (ICE) is their limited operability below a minimum rotational speed. Starting an engine involves accelerating it up to a specific minimal speed of operation. Due to its inertia and the low starter power, a conventional start of an ICE takes up to 1 second. An engine shutdown during idling phases implying such long start times is not accepted by the driver. Therefore, conventional ICE are typically not shut down during idling phases.

However, idling losses constitute a significant amount of the total fuel consumption. During the New European Driving Cycle (NEDC), they amount to 4-8% depending on the engine type and size as shown in [1-4]. In order to exploit this fuel saving potential by eliminating the idling phases while still satisfying driver demands, the duration of an engine start needs to be reduced.

A common approach to reducing the engine start time is the installation of a powerful Electric Starter (ES) and an appropriate battery. This strategy can be pursued with hybrid electric vehicles since they are equipped with more powerful electric motors and batteries than conventional engines. However, they induce additional weight and cost. In [5], it is shown that for this setup start times as low as 300 ms are achievable.

Several authors, *e.g.* those of [3, 6-8], investigated a method for fast starts of gasoline engines with direct fuel injection. The idea behind that approach is to inject fuel into the stopped engine. If the engine has stopped at an appropriate position, the fuel can be ignited at standstill to restart the engine without using the ES. However, a controlled engine shutdown is essential to enforce the engine to stop at an appropriate position. Robustness under all operating conditions and emissions due to incomplete combustion at low engine speeds are critical issues with this approach. The authors of [5] extended the investigation to ES-assisted engine starts to reduce the start time and the emissions.

A cost and weight effective alternative is to use compressed air that can be injected directly into the cylinders. The compressed air is stored in a tank. The tank can be recharged by running the engine as a piston compressor (as *e.g.* done in hybrid pneumatic engines [1]) or by an additional compressor which can be engaged to the crank shaft or which is driven electrically. For the rest of the paper, it is assumed that the compressed air is available and the recharging method is not discussed any further. Figure 1 shows a schematic representation of the engine setup considered. Figure 2 shows the setup of the engine on the testbench on which the measurements presented later in this paper are performed.

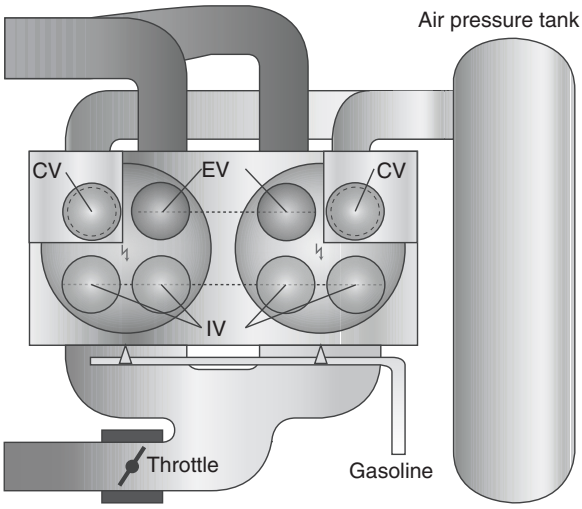

Figure 1

Schematic illustration of the engine setup. A two-cylinder engine with one Exhaust Valve (EV) and two Intake Valves (IV) per cylinder is shown. One EV per cylinder is replaced by a Charge Valve (CV).

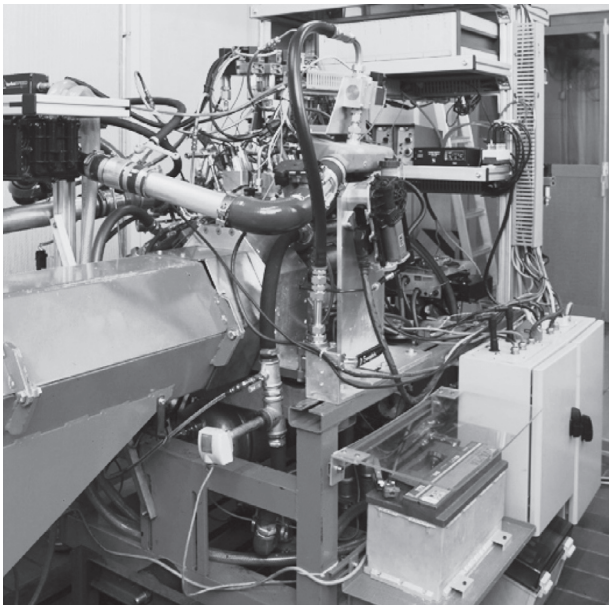

Figure 2

Photograph of the engine including the testbench equipment on which the measurements presented in this paper are performed.

To start the engine pneumatically, air is injected during the expansion stroke where it produces a positive torque that accelerates the engine. The engine is then

driven purely pneumatically without burning any fuel. In [9], pneumatic engine starts using a fully variable valve system for the actuation of the charge valves (CV) are investigated. Using this setup, the CV lift profile can be adapted on a cycle-to-cycle basis. However, a fully variable valve system increases the complexity and cost of the system.

In this paper, pneumatic engine starts using camshaft driven CV are investigated. Camshaft driven CV are characterized by a valve lift profile which cannot be adapted during the operation of the engine. The CV lift profile must be defined during the design process. Furthermore, the camshaft driven valve system has an on/off capability, *i.e.* the valves can either be activated or deactivated. The level of complexity can be significantly reduced by using camshaft driven CV instead of fully variable CV. The goal of this work is to provide a methodology for the optimization of the CV design for minimum air consumption with the constraint of a maximally allowable engine start time. Parts of this work were already presented in [10], the content of which was revised and extended with a detailed system analysis for various operating conditions.

The paper is structured as follows: in Section 1, the model and the setup of the engine as well as the boundary conditions for the optimization of the CV design are introduced. Additionally, an engine stop strategy is proposed. In Section 2, the design problem is formulated as a constrained minimization problem. A design methodology to solve this optimization problem is presented. Section 3 shows the application of this methodology in a design example whose results are verified experimentally on a test bench engine. The CV design found is analyzed with respect to varying initial engine positions, tank pressures and tank temperatures. The paper finishes with a conclusion summarizing the contribution of this work and an outlook on future research.

1 MODEL AND SETUP

For the determination of the optimal CV parameters a process model of the engine is used to simulate the start. A detailed description of the model can be found in Appendix A. This section deals with the electric starter, the parameters of the valve lift profile and the role of the initial engine position. The influence of the pneumatic start on the catalyst temperature is a practical issue which is briefly discussed in Appendix B.

Note that for the crank angle $\phi = 0°$, the piston is located at the Top Dead Center (TDC) after the compression stroke. Crank angles with values of $\phi > 0°$ are located after TDC.

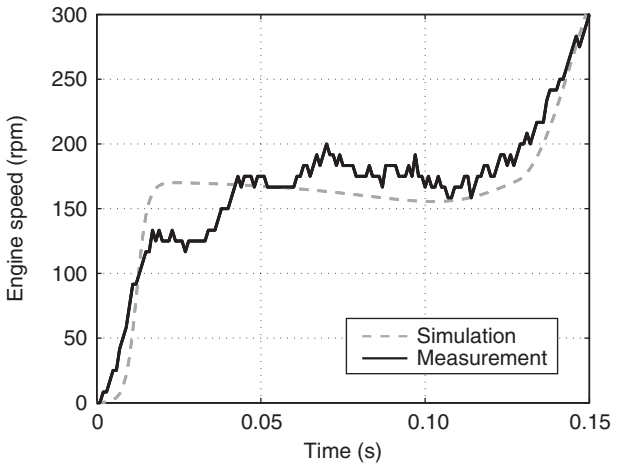

Figure 3

Graph of the measured and simulated engine speed during an engine start (first half of the first engine revolution, where the ES is active). The measurements are taken on the engine described in Section 3.

1.1 Electric Starter

In contrast to [9], this paper focuses on camshaft driven CV. In such a realization, the valve lift profile is fixed. Furthermore, the valve can only be actuated by a rotating engine. For the initial actuation of the CV and for other reasons as described in [7] an ES is essential. Furthermore, the ES helps to reduce the start time since it serves as an additional torque supplier during the pneumatic engine start.

In order to precisely predict the behavior of the engine during the start phase, a good model of the ES is crucial. Since the operation of the ES takes place under highly dynamic conditions, the model of the ES needs to be identified during transient operation. The behavior of the ES is modeled as a static torque-speed relationship $T_{ES}(\omega_e)$ for engine speeds below 200 rpm. For higher engine speeds the engine and the ES are assumed to be disconnected. A least squares approach is used to find a polynomial fit for the torque-speed relationship. Figure 3 shows the experimental validation of the relationship found by contrasting the simulated and the measured engine speed trajectories. Only the first half of the first engine revolution is shown because in this phase the dynamics of the ES are dominant.

1.2 Valve Lift Profile

The valve lift profile is assumed to have a simplified valve acceleration profile in the Crank Angle (CA) domain, *i.e.*

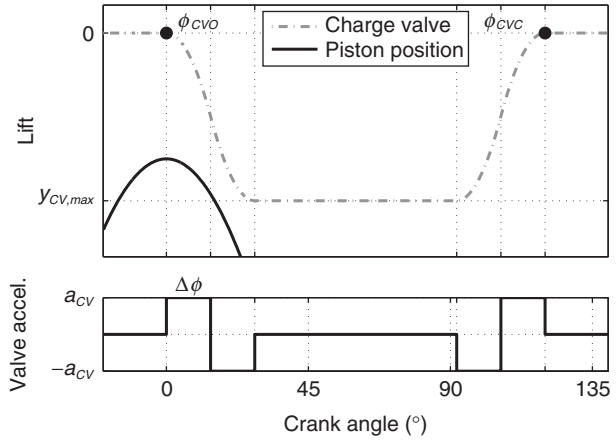

Figure 4

Sample CV lift and acceleration profile.

the magnitudes of the acceleration and the deceleration are equal and piecewise constant. Accordingly, the valve lift profile $y_{CV}(\phi)$ becomes a function of the acceleration in the CA domain a_{CV}, the CV opening angle ϕ_{CVO}, the CV closing angle ϕ_{CVC} and the maximum valve lift $y_{CV,max}$ that can be performed with the actuator chosen. The angular durations of the acceleration crenels are:

$$\Delta\phi = \sqrt{\frac{y_{CV,max}}{a_{CV}}} \tag{1}$$

To avoid the collision of the valve with the piston the following condition must be fulfilled:

$$y_{CV}(\phi) \leq \min\left\{\frac{V_{cyl}(\phi)}{A_{cyl}}, y_{CV,max}\right\} \tag{2}$$

where $V_{cyl}(\phi)$ is the cylinder volume at the CA position ϕ and A_{cyl} is the cross-sectional area of the cylinder. Figure 4 shows a sample CV lift profile.

To minimize throttling losses across the CV, the valve should be opened and closed as fast as possible. The valve acceleration thus has to be maximal. In contrast to the Intake Valves (IV) and the Exhaust Valves (EV), the CV is only actuated at low engine speeds. Since mechanical stresses apply in the time domain, the maximum CV acceleration in the CA domain can be chosen higher than that of the IV and EV. A reasonable value for the CV acceleration a_{CV} can be found with:

$$a_{CV} = a_{IV} \cdot \left(\frac{\omega_{e,max}}{\omega_{e,s,max}}\right)^2 \tag{3}$$

where a_{IV} denotes the IV acceleration in the CA domain, $\omega_{e,max}$ is the maximum engine speed and $\omega_{e,s,max}$ is the maximally allowable engine speed during the pneumatic start operation.

Given the maximum lift and the valve acceleration, the remaining parameters of the CV lift profile are ϕ_{CVO} and ϕ_{CVC}. A methodology to find appropriate values is presented in Section 2.

1.3 Initial Engine Position

The duration of the pneumatic engine start strongly depends on the time that elapses until pressurized air is injected for the first time. The sooner pressurized air is injected, the faster the engine starts. The duration until the CV opens at ϕ_{CVO} is mainly influenced by the size of the ES and the initial engine position ϕ_0. Hence, the engine should be shut down in a way such that the piston which is in the compression stroke comes to rest closely to the CV opening angle.

The rest position can be influenced by the amount of air that is sucked into the cylinder during the intake stroke. A higher air mass inside the cylinder results in more compression work to be done during the compression stroke. Hence, the piston comes to rest more closely to the Bottom Dead Center (BDC). For smaller air masses inside the cylinder the gas spring force induced by the compression is smaller resulting in piston rest positions closer to TDC.

The actuation of the throttle during the engine shutdown can be used to limit the pressure in the intake manifold and thus to adjust the amount of air that enters the cylinders. For engines equipped with a variable valve timing system, the variability of the opening duration of the IV can also be used to adjust the amount of air inside the cylinders.

Since the engine considered in this paper (for details, see Sect. 3) is not equipped with a variable valve timing system for the IV, the throttle is used to adjust the engine rest position. To find an appropriate value for the initial engine position in the model, several experiments are conducted. Several engine shutdowns with constant throttle opening are performed on the warmed-up engine and the rest position is recorded. The shutdowns are initialized at the engine's idling speed of 1 200 rpm. Figure 5 shows the results for the two-cylinder parallel twin engine considered. The best performance is achieved with a throttle opening of 2% because the variance is smallest and the mean position is closest to the TDC. Higher values yield a rest position which is further away from the TDC. Smaller throttle opening values yield a poor repeatability of the rest position, which is not

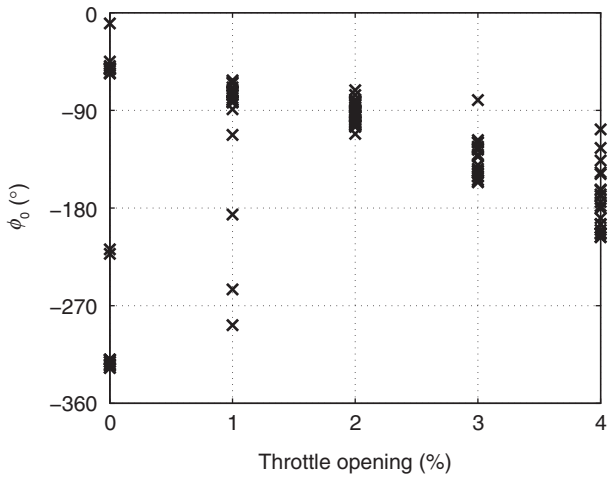

Figure 5

Measured engine rest positions for various throttle openings during engine shutdown. For details concerning the engine see Section 3.

desirable. Thus, an initial position of $\phi_0 = -95°$ CA is chosen.

1.4 Throttle Control during Engine Start

The throttle position setting found above is only relevant during engine shutdown. As shown in [9], completely closing the throttle during the engine start phase is air- and time-optimal. A closed throttle implies that the intake manifold pressure decreases during the start. Hence, the amount of air inside the cylinder is reduced, which causes less compression work to be required. Minimizing the compression work results in minimal negative torque during the engine start, which leads to shorter start times. Therefore, for the design methodology described below the throttle is always assumed to be completely closed during the engine start.

If a variable valve timing system for the IV is available, the compression work is minimized by setting the opening duration of the IV to the minimum.

2 DESIGN METHODOLOGY

In this section, the underlying optimization problem of the CV design is stated. The optimization problem is analyzed and discussed. A stepwise procedure for its solution is presented. The feasible set satisfying all the constraints is determined and specific design choices are introduced.

The objective of the proposed design methodology is to find values for the design variables which enable the engine to reach a prescribed start speed $\omega_{e,s}$ within less than a prescribed start time $t_{s,max}$ and which at the same time minimize the amount of pressurized air used. The relevant design variables are: ϕ_{CVO}, CV opening angle, ϕ_{CVC}, CV closing angle, d_{CV}, CV diameter.

Let $\Delta = \{\phi_{CVO}, \phi_{CVC}, d_{CV}\} \in \mathbb{R} \times \mathbb{R} \times \mathbb{R}^+$ be the parameter space considered for the relevant design variables. The variable δ denotes a single design in the set Δ.

The start time and the air consumption also depend on the initial tank pressure p_t. During the operation of the engine on a drive cycle, the tank pressure varies. The variation of the tank pressure is induced by the emptying and recharging of the tank caused by operating modes that use or provide pressurized air, respectively. Fully variable valves can adjust their valve timing to account for the changing tank pressure. However, the valve timing of camshaft driven CV is fixed. Hence, the design procedure has to consider the entire operating range of the tank pressure. To that end, the weighted sum of the amounts of air consumption resulting for n different tank pressures $\vec{\mathbf{p}}_t \in \mathbb{R}^{n,+}$ is minimized.

The tank temperature impacts the start time and the air consumption as well, due to its influence on the mass transfer into the cylinders. However, for the proposed design methodology the tank temperature is assumed to be constant due to the following reasons. According to Equation (A2) the mass flow only depends on the square root of the tank temperature in contrast to the tank pressure on which the mass flow depends linearly. Furthermore, the relative temperature change of the air tank during the operation of the engine is significantly smaller than the relative tank pressure change. Due to the uninsulated tank, the temperature varies according to measurements between 10°C and 50°C or 283 K and 323 K, respectively, *i.e.* $\pm 7\%$, whereas the tank pressure varies between 6 bar and 14 bar, *i.e.* $\pm 40\%$. The influence of the air temperature in the tank on the resulting optimal CV design is analyzed in Appendix C. It turns out that the assumption of a constant air temperature in the tank is justified.

Considering only the variation in the tank pressure, the optimization problem can be written as:

$$\min_{\delta \in \Delta} \sum_{i=1}^{n} w(\vec{\mathbf{p}}_t(i)) \cdot m_a(\delta, \vec{\mathbf{p}}_t(i)) \;\text{ s.t. }\; t_s(\delta, \vec{\mathbf{p}}_t(i)) \leq t_{s,max} \tag{4}$$

where $w(\vec{\mathbf{p}}_t(i))$ are the pressure dependent weighting factors, t_s is the time needed to reach the desired engine speed $\omega_{e,s}$ and m_a denotes the amount of air used for

the start. The values of t_s and m_a are calculated with the nonlinear process model f_{PM}:

$$[m_a(\delta, p_t), t_s(\delta, p_t)] = f_{PM}(\delta, p_t, \omega_{e,s}) \tag{5}$$

The air consumption m_a is calculated by taking the integral over the mass flow through the CV $\dot{m}_{CV}$:

$$m_a = \int_0^{\hat{t}_s} \dot{m}_{CV}\, dt \tag{6}$$

where $\hat{t}_s$ implies an extension of the integration interval to $\hat{t}_s \geq t_s$. It is defined as the smallest value of $\hat{t}_s$ satisfying the following constraints:

$$\omega_e(\hat{t}_s) \geq \omega_{e,s} \tag{7}$$

$$\dot{m}_{CV}(\hat{t}_s) = 0 \tag{8}$$

Hence, the variable $\hat{t}_s$ defines the instant when the CV are closed and the pneumatic start is completed. This definition accounts for the fact that the CV cannot be closed and deactivated immediately when $\omega_e = \omega_{e,s}$ is reached. In contrast to the fully variable valves used in [9], the camshaft driven CV can only be deactivated if $\phi \notin [\phi_{CVO}, \phi_{CVC}]$. Figure 6 visualizes the definitions of t_s and $\hat{t}_s$ for a pneumatic engine start.

The scalar weighting function $w(p_t) \geq 0$ only depends on the initial tank pressure. It is used to select and penalize specific initial tank pressures in the optimization. Promoting high initial tank pressures results in an inferior design for low initial tank pressures and *vice versa*. A reasonable choice of $w(p_t)$ is to make it large at low initial tank pressures. For low initial tank pressures, the air consumption can become a critical issue during a drive cycle. On the other hand, if the initial tank pressure is high, an increased air consumption can be accepted. Special attention should be paid to frequently occurring initial tank pressures during the drive cycle.

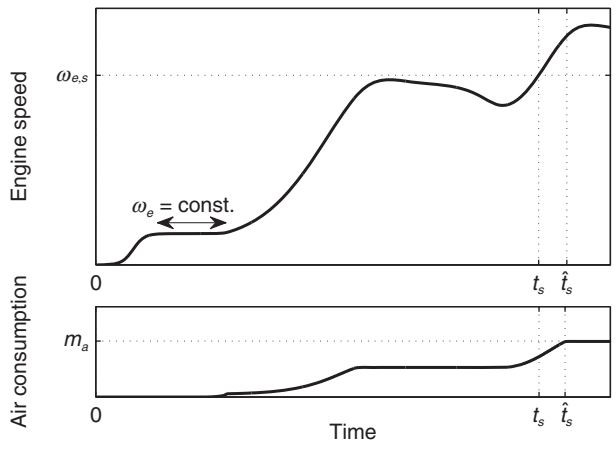

Figure 6

Engine speed and cumulative air consumption for a pneumatic engine start. During the constant speed phase, the engine is only driven by the ES. The variables t_s and $\hat{t}_s$ are labeled to clarify their definitions.

2.1 Properties of the Optimization Problem

Due to the reciprocating behavior of the engine and the highly nonlinear process model f_{PM} the optimization problem has special features. These are discussed below.

The feasible set is defined as:

$$\Omega(p_t) := \{\Delta | t_s(\Delta, p_t) \leq t_{s,max}\} \tag{9}$$

i.e., it contains all designs which fulfill the performance constraint for the initial tank pressure p_t. The smallest initial tank pressure for which $\Omega(p_t)$ is not empty is defined as the minimum tank pressure $\tilde{p}_{t,\Omega}$ of the feasible set. The tank pressures considered have to fulfill the inequality $\vec{\mathbf{p}}_t(i) \geq \tilde{p}_{t,\Omega}\, \forall i$. However, since the minimum tank pressure is not known *a priori*, the choice of $\vec{\mathbf{p}}_t$ is difficult. This fact makes it also difficult to formulate a reasonable weighting function $w(p_t)$, which ensures that the correct tank pressure range is promoted or penalized.

Furthermore, the reciprocating behavior of the engine implies a further difficulty for the solution of the optimization problem. The function $[m_a, t_s] = f_{PM}$ is piecewise continuous in both the air mass and the start time. This fact is shown by introducing the following consideration. Let δ_1 and δ_2 be two designs with $||\delta_1 - \delta_2||_\infty < \varepsilon$ where $||\cdot||_\infty$ denotes the infinity norm and $\varepsilon > 0$ is a very small number. Hence, the two designs differ just slightly. However, for specific choices of δ_1 and δ_2 the evaluation of $f_{PM}(\delta_i, p_t)$ for the same initial tank pressure yields completely different results. Such a discrepancy occurs when $\omega_{e,s}$ is reached in different numbers of power strokes: $N_{ps}(\delta_1) \neq N_{ps}(\delta_2)$. Thus, there is a discontinuity in m_a and t_s between δ_1 and δ_2. Discontinuities in the objective function can cause problems with numerical optimization algorithms. Further details on this discontinuity property are shown in Section 3.3 for a design example.

2.2 Solution to the Optimization Problem

Depending on the objective of the optimization and the prior knowledge two solving methods are proposed, namely numerical optimization and a brute-force approach. For the numerical optimization, the Particle

TABLE 1
Comparison of the solving methods

Method	Numerical optimization	Brute-force
Min. tank pressure	Must be known	Is found
Calculation time	Fast	Slow
Precision of solution	High	Lower
Sensitivity analysis	Not suited	Suited

Swarm Optimization (PSO) is proposed since it copes well with the properties of the problem described above. Table 1 lists the properties of the proposed methods. The numerical optimization is suited if the minimum tank pressure is known, such that $\vec{\mathbf{p}}_t$ can reasonably be selected. The derivation of the optimal solution is rather fast, and a precise solution is found.

In the brute-force approach the process model is simulated for a multitude of CV design variables and tank pressures. It is computationally more demanding. Of course, the computational demand depends on the coarseness of the considered grid. The advantage of this method lays in the fact that the minimum tank pressure does not need to be known in advance. It is found within the approach. Furthermore, the simulation results can be used for sensitivity analyses. The precision of the solution is limited by the coarseness of the grid.

In the following, the two solution methods are explained. Regardless of the solving method, the specifications, *i.e.* $\omega_{e,s}$ and $t_{s,max}$, have to be formulated first.

2.2.1 Numerical Optimization

If the minimum tank pressure $\tilde{\mathrm{p}}_{t,\Omega}$ is known, a reasonable tank pressure range $\vec{\mathbf{p}}_t$ and a reasonable weighting function can be defined. For the solution the PSO algorithm presented in [11] is proposed.

2.2.2 Brute-Force

The brute-force approach visualized in Figure 7 starts with the definition of a grid $\Gamma = \{\Delta, p_t\}$ on which the process model is evaluated. Then, the evalution of the process model on Γ follows. The computational effort for the evaluation depends on the discretization chosen. Given $t_s(\Gamma) = f_{PM}(\Gamma, \omega_{e,s})$, the feasible set Ω and the minimum tank pressure $\tilde{p}_{t,\Omega}$ can be derived. A reasonable tank pressure range $\vec{\mathbf{p}}_t$ and a reasonable weighting function thus can be defined.

The optimal solution $\delta^* = \{\phi^*_{CVO}, \phi^*_{CVC}, d^*_{CV}\}$ is found by evaluating Equation (4) on the feasible set Ω. This

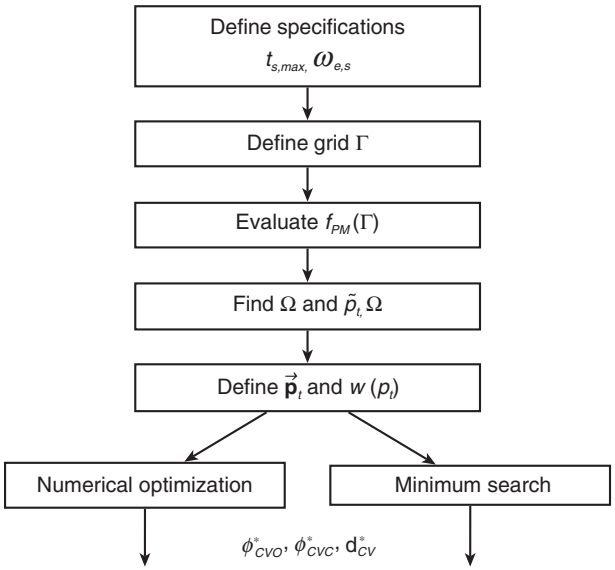

Figure 7
CV design procedure for pneumatic engine start.

minimum search is computationally not demanding if $\vec{\mathbf{p}}_t \in \Gamma$, *i.e.*, if $\vec{\mathbf{p}}_t$ consists only of tank pressures that are also part of Γ. Then, no further model evaluations are necessary. Alternatively, a numerical optimization can be conducted with the defined tank pressure range and weighting function. It is computationally more demanding than the minimum search on an already existing grid. However, the solution is more precise.

3 DESIGN EXAMPLE

The following design example shows the application of the CV design methodology presented. The engine under consideration is a two-cylinder parallel twin engine. For more details on the engine, see [9] where the same engine was used. The specifications of the engine are given in Table 2. The maximum CV lift is $y_{CV,max} = 4\,\mathrm{mm}$, which corresponds to the value that can be performed on the test bench engine. The IV acceleration a_{IV} that guarantees safe operation up to the maximum engine speed $\omega_{e,max}$ is given in Table 2. By applying Equation (3), the maximally allowable CV acceleration in the CA domain is found to be $a_{CV} = 3.04 \times 10^{-5}\mathrm{m}/^{\circ}\mathrm{CA}^2$.

Specifications

The desired start engine speed is set to $\omega_{e,s} = \omega_{e,idle} = 1\,200\,\mathrm{rpm}$. The maximally allowable start

TABLE 2
Design example parameterization

Parameter	Variable	Value	Unit
Number of cylinders	N_{cyl}	2	–
Displacement	V_d	0.75	l
Bore diameter	B	85	mm
Stroke	S	66	mm
Connecting rod	l	115	mm
Compression ratio	ε	9	–
Idling speed	$\omega_{e,idle}$	1 200	rpm
Max. engine speed	$\omega_{e,max}$	6 000	rpm
Max. start engine speed	$\omega_{e,s,max}$	1 500	rpm
Number of IV per cyl.	N_{IV}	2	–
Number of EV per cyl.	N_{EV}	1	–
Number of CV per cyl.	N_{CV}	1	–
IV closing CA	ϕ_{IVC}	–114	°CA
EV opening CA	ϕ_{EVO}	114	°CA
IV acceleration	a_{IV}	0.19×10^{-5}	m/°CA^2
CV acceleration	a_{CV}	3.04×10^{-5}	m/°CA^2
CV diameter	d_{CV}	19.0	mm
Maximum valve lift	$y_{CV,max}$	4.0	mm
Initial engine position	ϕ_0	–95	°CA
Tank volume	V_t	30	l
Tank temperature	ϑ_t	50	°C

TABLE 3
Grid Γ used in the design example.

Variable	Lower bound	Upper bound	Step size
ϕ_{CVO}	–110°CA	50°CA	10°CA
ϕ_{CVC}	60°CA	220°CA	10°CA
d_{CV}	7 mm	21 mm	2 mm
p_t	7 bar	12 bar	1 bar

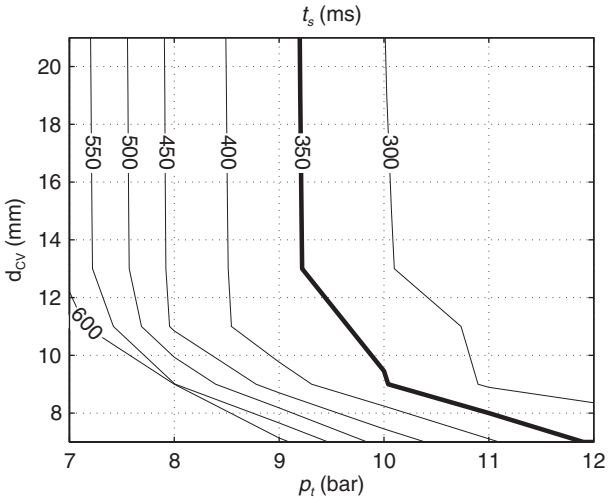

Figure 8

Minimum start time for various CV diameters and initial tank pressures.

time is chosen as $t_{s,max} = 350$ ms. These specifications are in accordance with the values used in [5] and [9].

Grid Definition

The grid Γ considered in the design example is given in Table 3.

Evaluation of the Process Model

In this step, the nonlinear process model f_{PM} is evaluated for Γ, which involves 13 872 model evaluations for the grid considered.

Determination of the Feasible Set and its Minimum Initial Tank Pressure

The analysis of the simulation results yields a minimum initial tank pressure of $\tilde{p}_{t,\Omega} \approx 9.2$ bar for $d_{CV} > 13$ mm. Figure 8 visualizes this result. It shows the minimum start time achievable for fixed combinations of d_{CV} and p_t. The bold 350 ms line indicates the boundary of the feasible set in the p_t-d_{CV} subspace. All combinations of initial tank pressures and CV diameters with $t_s \leq 350$ ms are part of the feasible set.

On the test bench, CV with a diameter of $d_{CV} = 19$ mm are installed. This diameter is thus chosen for the design example and kept as a fixed value throughout the rest of the optimization procedure.

Definition of the Tank Pressure Range and the Weighting Function

Based on the data depicted in Figure 8 the tank pressure vector $\vec{\mathbf{p}}_t$ can be defined. In this example, only one tank pressure close to the boundary of the feasible set is considered. Thus, no weighting is necessary:

TABLE 4
Optimal values of the design variables for $d_{CV} = 19\,\text{mm}$ and $p_t = 10\,\text{bar}$

	Minimum search	PSO
ϕ^*_{CVO}	10°CA	13.7°CA
ϕ^*_{CVC}	110°CA	110.1°CA
m^*_a	10.15 g	10.13 g
t^*_s	350 ms	350 ms
N^*_{ps}	4	4

$$\vec{\mathbf{p}}_t = \{10\ \text{bar}\},\ w(p_t) = 1 \tag{10}$$

Minimum Search and Numerical Optimization

According to the procedure described in Section 2, the optimal CV design can be found by a minimum search on the feasible set. Since the tank pressure considered is on the grid, no further simulations are necessary. Table 4 lists the values for the design variables found by the minimum search and the PSO, respectively, for $d_{CV} = 19\,\text{mm}$ and $p_t = 10\,\text{bar}$. The resulting valve timings found with the two methods are very close to each other. The resulting start time is 350 ms. Thus, the maximum start time is fully exploited, and the solution lies on the boundary of the feasible set. The number of power strokes required to start the engine is $N_{ps} = 4$.

Figure 9 shows the air consumption for the relevant part of $\{\phi_{CVO}, \phi_{CVC}\} \in \Gamma$ and a tank pressure of 10 bar.

3.1 Discussion

The optimization procedure yields a CV opening angle after TDC. This result is advantageous because the first engine revolution would become critical if the CV was to be opened before TDC and the initial tank pressure was large, *i.e.* significantly larger than the in-cylinder pressure at TDC. In that case, a negative torque would be produced by the injection of pressurized air before the piston passes TDC. If this torque exceeded the torque produced by the ES, the engine could not be started pneumatically.

Figure 9 clearly shows that a later closing of the CV is unfavorable with respect to the air consumption. The reason for this fact is that the opening angle of the EV is at $\phi = 114$°CA. A design where $\phi_{CVC} > 114$°CA implies that pressurized air flows from the CV directly into the exhaust manifold. Such a design increases the air consumption without producing significantly higher torques.

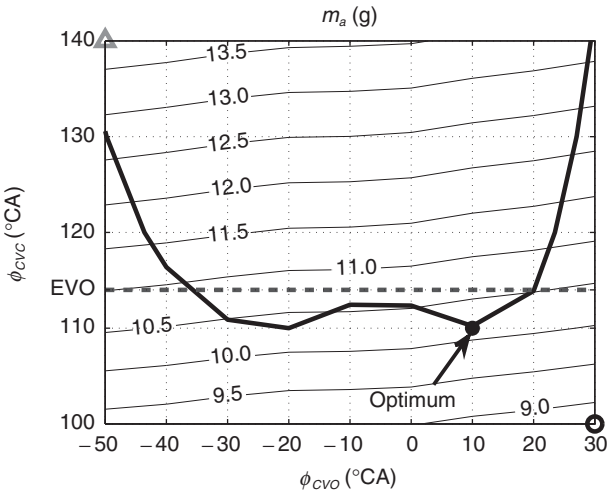

Figure 9

Consumption of pressurized air for various CV opening and closing angles with $d_{CV} = 19\,\text{mm}$ and $p_t = 10\,\text{bar}$. The black bold line denotes the boundary of the feasible set. The label EVO denotes the EV opening angle. Black circle: minimum air consumption. Gray triangle: maximum air consumption.

Sensitivity Analysis

Based on the results depicted in Figures 8-10, a sensitivity analysis of the parameters in the set Γ can be performed.

Figure 8 shows that for small CV diameters the minimum tank pressure to satisfy $t_s \leq t_{s,max}$ increases significantly. For small values of d_{CV} less air can be transferred through the CVs due to the flow restriction. Thus, the torque is lower. The increased flow restriction needs to be compensated by a higher density, *i.e.* a higher tank pressure. For $d_{CV} > 14\,\text{mm}$, the start time is almost constant for a fixed tank pressure. Larger values of d_{CV} might be expected to result in more air being transferred and hence in reduced start times. However, there is a counteracting effect. For large valve diameters, the pressure difference between tank and cylinder decreases rapidly once the CV is opened. This effect results in a reduction of the mass flow rate.

Figure 10 shows the start time for various combinations of ϕ_{CVO} and ϕ_{CVC} for fixed values of $p_t = 10\,\text{bar}$ and $d_{CV} = 19\,\text{mm}$. The maximum start time on the grid shown is equal to 370 ms, and it is indicated by a gray triangle. The minimum start time is 341 ms and is indicated by a black circle. Thus, the maximum start time is 8% higher than the minimum start time, which indicates a rather small sensitivity. Around TDC, the start time t_s is almost constant for varying CV opening angles.

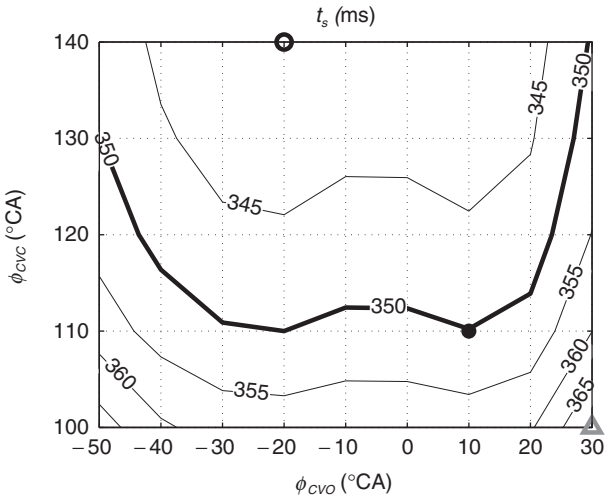

Figure 10

Start times for various CV opening and closing angles for $p_t = 10$ bar and $d_{CV} = 19$ mm. The bold black line denotes the boundary of the feasible set where all combinations above the line are feasible. Black circle: minimum start time. Gray triangle: maximum start time.

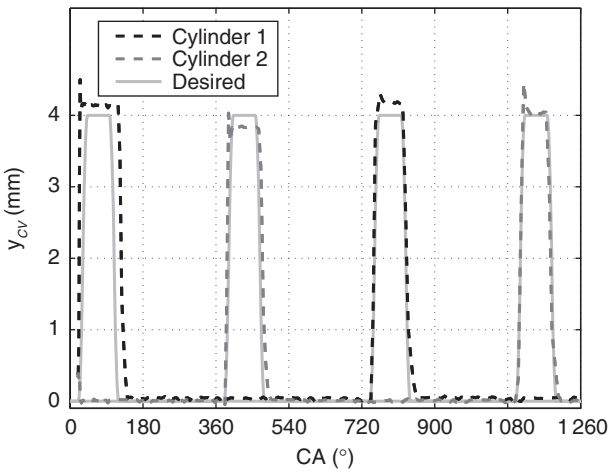

Figure 11

Desired and emulated CV lift profiles.

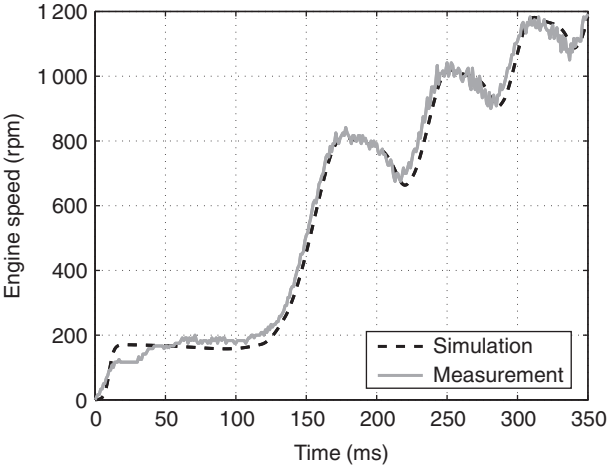

Figure 12

Measured and simulated pneumatic engine start.

On the other hand, the start time can be reduced by a later closing of the CV.

The air consumption depicted in Figure 9 shows a rather high sensitivity to the CV timing. In the CV timing intervals depicted, the minimum air consumption is 8.7 g (black circle). The maximum air consumption amounts to 13.8 g (gray triangle), which is 58% larger. Analogously to the start time, around TDC there is a small variation of m_a in terms of the CV opening angle. However, the gradient of the air consumption as a function of the CV closing angle points in the opposite direction of the gradient of the start time.

These results allow the conclusion that a later closing of the CV implies shorter start times but an increased air consumption. Comparing the time optimal and air optimal designs within the grid considered indicated by the black circles in Figures 9 and 10 leads to the statement that accepting an increase in the start time by 8% results in an air saving of 36%.

3.2 Experiments

In order to verify the quality of the model and the CV design found, the pneumatic start is implemented on a test bench engine with the optimal CV timings obtained from the design example. The CV are actuated by a fully variable valve system which allows the emulation of a wide variety of CV lift profiles. Figure 11 shows the desired and the emulated CV lift profiles of both cylinders for the engine start shown in Figure 12.

Figure 12 shows the engine speed trajectories for a measured and a simulated pneumatic start. The limit of $t_s = t_{s,max} = 350$ ms is fully exploited, which corresponds to the result predicted by simulation and presented in Table 4. The pressure drop in the air tank over the entire pneumatic engine start phase is approximately 300 mbar. The corresponding air mass consumption is 10.5 g, which agrees with the value predicted by the process model. The discrepancy is 3%.

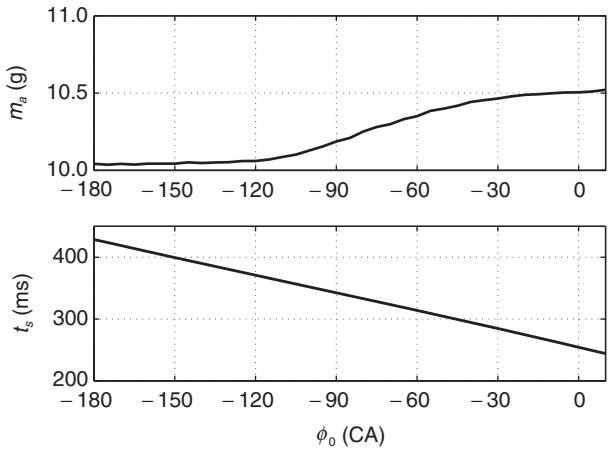

Figure 13

Air consumption and start time for various initial engine positions ϕ_0 for $\phi^*_{CVO} = 10°\text{CA}$, $\phi^*_{CVC} = 110°\text{CA}$, $d_{CV} = 19\,\text{mm}$ and $p_t = 10\,\text{bar}$.

Only four power strokes are required to reach the desired final engine speed $\omega_{e,s} = \omega_{e,idle} = 1\,200\,\text{rpm}$. During the first third of the start time, the engine is driven only by the ES until ϕ_{CVO} is reached. This duration can only be reduced by a more powerful ES.

The good agreement between measurement and simulation data confirms the quality of the process model.

3.3 System Analysis

3.3.1 Influence of the Initial Engine Position

The throttle strategy during the engine shutdown presented in Section 1.3 showed reliable results on the test bench. In this section, the importance of the initial engine position is highlighted by simulating the engine start for various initial positions. Figure 13 shows the resulting air consumption and start time data as a function of the initial engine position ϕ_0. If the start is initiated closer to the CV opening position the start time is shorter because it takes less time until pressurized air is injected and, thus, a high torque is applied. Furthermore, the first CV opening lasts longer since the engine speed is low. Hence, more air is injected, which yields a higher torque. The influence of the start position on the start time is significant. If the engine is started from the BDC position, it takes 430 ms. The start from the TDC position takes just 259 ms, which is faster by 40%.

In contrast, the air consumption is not very sensitive to the initial engine position. For the start positions considered, an increase of just 5% can be observed. The air consumption is rather constant for start positions from $\phi = -180°\text{CA}$ to $\phi = -120°\text{CA}$. This can be explained by the open IV, through which air is blown out. The air consumption is highest if the initial position is just before the CV opening because in this case the engine speed and the cylinder pressure are rather low during the first air injection. Hence, the CV is open for a very long time and a lot of compressed air is injected.

In conclusion, a good positioning of the engine during the shutdown substantially influences the start time while the air consumption is affected only slightly.

3.3.2 Variation of the Initial Tank Pressure

During the operation of the engine, the tank pressure varies due to emptying and refilling of the air pressure tank. In this section, the start performance of camshaft driven CV with respect to the air used and the start duration is analyzed for various initial tank pressures. The analysis is conducted for the optimal CV design with $\phi^*_{CVO} = 10°\text{CA}$ and $\phi^*_{CVC} = 110°\text{CA}$ using the process model f_{PM}. Figure 14 shows the results. The first subplot shows the total amount of air used, m_a, and the amount of air used when the desired engine speed is reached $m_a(t_s)$. The second subplot shows the start time t_s and the time $\hat{t}_s$ when the valves are closed. The third subplot shows the number of power strokes N_{ps} required to reach the desired engine speed.

As stated in Equation (6), the amount of air used to start the engine is calculated as the integral of the air mass flow. Therefore, the same amount of air is used whether a larger mass flow occurs for a short time or whether a small mass flow exists for a longer time duration. For instance, the air consumptions for initial tank pressures of $p_t = 9.3\,\text{bar}$ and $p_t = 12\,\text{bar}$, respectively, are equal. However, the start times are different.

Obviously, a higher tank pressure leads to a higher air mass flow. The torque exerted is larger, which leads to a shorter start time t_s. The total amount of air m_a used for an engine start is a piecewise continuous function of the tank pressure. The steps occur when the number of power strokes changes. For an equal number of power strokes the amount of air used increases along with an increasing tank pressure mainly because the valve cannot be closed when the desired engine speed is reached. If a CV is available that can be deactivated immediately the air consumption can be reduced to $m_a(t_s)$. However, the piecewise continuity remains.

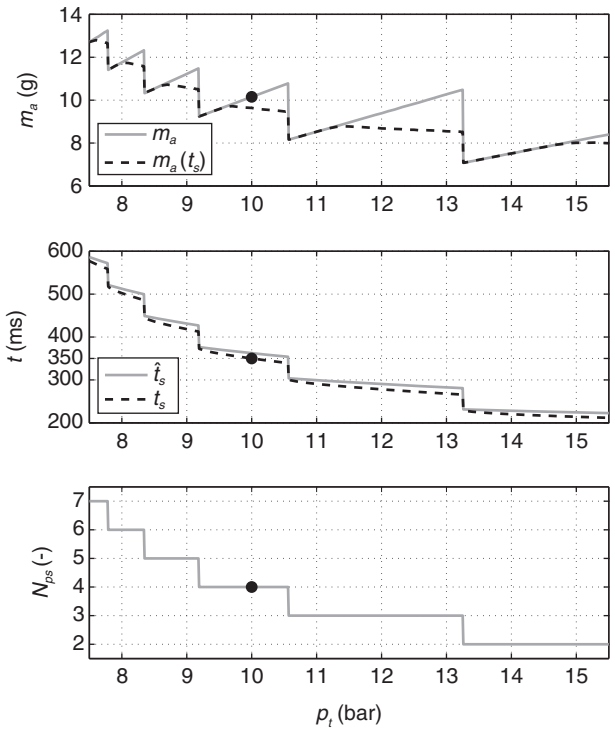

Figure 14

Air consumption, start time and number of power strokes for various tank pressures for $\phi^*_{CVO} = 10°$ CA, $\phi^*_{CVC} = 110°$ CA and $d_{CV} = 19$ mm. The black dot indicates the optimal result of the design example.

CONCLUSION

A general design methodology for camshaft driven charge valves used for pneumatic engine starts is presented. The design procedure is exemplified for a two-cylinder engine, and the results are verified experimentally. The discrepancy between the results predicted and those obtained on the testbench is 3%.

Pneumatic engine starts enable significantly reduced engine start times compared to those of conventionally started engines. In contrast to conventional engine starts, a large positive torque is produced already during the first expansion stroke. Another advantage of pneumatic engine starts is the fact that they are applicable on engines with port fuel injection as well as on those with direct injection. Starting the engine without burning any fuel also reduces the emission of hydrocarbons and carbon-monoxide which are caused by the incomplete combustion occurring at very low engine speeds.

In summary, pneumatic engine starts offer the possibility to implement stop/start strategies that satisfy the comfort demands of the driver without significantly increasing the complexity and cost of the whole engine system.

OUTLOOK

The pneumatic engine start treated in this paper was investigated on a gasoline engine with port fuel injection. However, the possibility to inject pressurized air directly into the cylinders offers additional advantages for engines with direct gasoline injection. As mentioned *e.g.* in [6] and [7], the direct start using fuel injection into the stopped engine suffers from the fact that a successful start is guaranteed only for a limited range of engine rest positions. The injection of pressurized air can be used to extend the range of initial engine positions where the direct engine start is guaranteed to be successful. Additionally, the pneumatically assisted engine start with early direct fuel injection can help to further reduce the start time. The combination of the pneumatic start and the direct start is being considered in ongoing research.

REFERENCES

1 Dönitz C., Vasile I., Onder C., Guzzella L. (2009) Dynamic Programming for Hybrid Pneumatic Vehicles, *American Control Conference*, 3956-3963.

2 Silva C., Ross M., Farias T. (2009) Analysis and Simulation of "Low-cost" Strategies to Reduce Fuel Consumption and Emissions in Conventional Gasoline Light-duty Vehicles, *Energy Conversion and Management*, 215-222.

3 Zülch C.D. (2007) Konzepte für einen sicheren Direktstart von Ottomotoren, *PhD Thesis*, University of Stuttgart.

4 Rau A. (2009) Analyse und Optimierung des Ottomotorischen Starts und Stopps für eine Start Stopp Automatik, *PhD Thesis*, Technical University of Clausthal.

5 Fesefeldt T., Müller S. (2009) Optimization and Comparison of Quick and Hybrid Start, *SAE Technical Paper* 2009-01-1340.

6 Kulzer A., Laubender J., Lauff U., Mössner D., Sieber U. (2006) Direct Start – From Model to Demo Vehicle, *MTZ Worldwide*. **67**, 9, 12-15.

7 Kramer U. (2005) Potentialanalyse des Direktstarts für den Einsatz in einem Stopp-Start-System an einem Ottomotor mit strahlgeführter Benzin-Direkteinspritzung unter besonderer Berücksichtigung des Motorauslaufvorgangs, *PhD Thesis*, University of Duisburg-Essen.

8 Ueda K., Kaihara K., Kurose K., Ando H. (2001) Idling Stop System Coupled with Quick Start Features of Gasoline Direct Injection, *SAE Technical Paper* 2001-01-0545.

9 Vasile I., Dönitz C., Voser C., Vetterli J., Onder C., Guzzella L. (2009) Rapid Start of Hybrid Pneumatic Engines, *Proceedings of the IFAC Workshop on Engine and Powertrain Control, Simulation and Modeling, E-COSM'09*, IFP Energies nouvelles, Rueil-Malmaison, France, 30 Nov.-02 Dec, pp. 123-130.

10 Moser M., Voser C., Onder C., Guzzella L. (2012) Design Methodology of Camshaft Driven Charge Valves for Pneumatic Engine Starts, *Proceedings of the IFAC Workshop on Engine and Powertrain Control, Simulation and Modeling, E-COSM'12*, IFP Energies nouvelles, France, 23-25 Oct., pp. 33-40.

11 Ebbesen S., Kiwitz P., Guzzella L. (2012) A Generic Particle Swarm Optimization Matlab Function, *Proceedings of the American Control Conference*, Montréal, Canada, 27-29 June, pp. 1519-1524.

12 Guzzella L., Onder C. (2010) *Introduction to Modeling and Control of Internal Combustion Engine Systems*, Springer, 2nd ed.

13 Pischinger R., Krassnig G., Taucar G., Sams T. (1989) *Thermodynamik der Verbrennungskraftmaschine*, Springer, Wien, New York.

Manuscript accepted in November 2013
Published online in April 2014

Cite this article as: M.M. Moser, C. Voser, C.H. Onder and L. Guzzella (2015). Design Methodology of Camshaft Driven Charge Valves for Pneumatic Engine Starts, *Oil Gas Sci. Technol* **70**, 1, 179-194.

APPENDIX A: PROCESS MODEL

The most important relations used in the process model f_{PM} are described in this appendix. The engine cylinders are modeled as receivers with variable volume. Every cylinder $i = \{1, ..., N_{cyl}\}$ has its crank angle position ϕ_i. For $\phi_i = 0°$ CA the piston is located at the TDC after the compression stroke.

Mass Balance

The air mass of every cylinder $m_{cyl,i}$ is determined by the mass flows $\dot{m}_{k,i}$ through each valve type $k = \{IV, EV, CV\}$:

$$\frac{dm_{cyl,i}(t)}{dt} = \dot{m}_{IV,i} + \dot{m}_{CV,i} - \dot{m}_{EV,i} \tag{A1}$$

Blow-by is neglected. According to [12] the mass flow through the valves is modeled as a compressible flow restriction:

$$\dot{m}_{k,i} = c_d \cdot A \cdot \frac{p_{up}}{\sqrt{R_a \cdot \vartheta_{up}}} \cdot \psi\left(\frac{p_{up}}{p_{down}}\right) \tag{A2}$$

where c_d denotes the discharge coefficient, A is the maximal opening area of the valve, p_{up} and p_{down} correspond to the upstream and downstream pressures, respectively, ϑ_{up} is the upstream temperature, R_a is the ideal gas constant of air and $\psi(.)$ is the flow function. For the discharge coefficient c_d the relation of [13] is used, where it is defined as a function of the relative lift y_{CV}/d_{CV}. Figure A1 shows the relations for all engine valves.

The flow function $\psi(.)$ is defined by:

$$\psi\left(\frac{p_{up}}{p_{down}}\right) = \begin{cases} \sqrt{\kappa\left[\frac{2}{\kappa+1}\right]^{\frac{\kappa+1}{\kappa-1}}} & \text{for } p_{down} < p_{cr} \\ \left[\frac{p_{down}}{p_{up}}\right]^{\frac{1}{\kappa}} \sqrt{\frac{2\kappa}{\kappa-1}\left[1 - \left(\frac{p_{down}}{p_{up}}\right)^{\frac{\kappa-1}{\kappa}}\right]} & \text{for } p_{down} \geq p_{cr} \end{cases} \tag{A3}$$

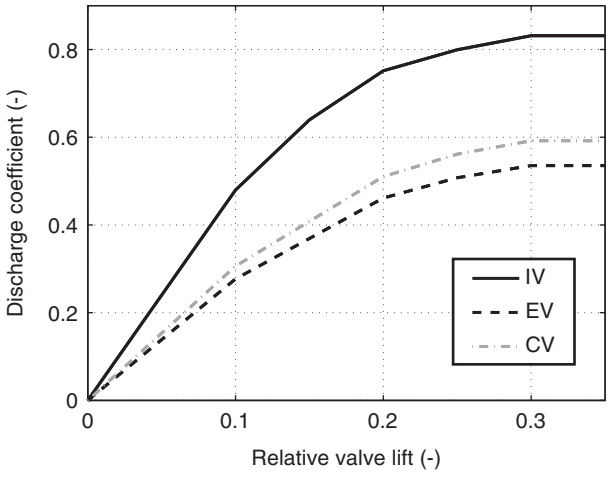

Figure A1

Discharge coefficient as a function of the relative valve lift. The relative valve lift is the ratio of the absolute valve lift and the valve diameter.

where κ is the ratio of the specific heats. The critical pressure p_{cr} at which the flow reaches sonic conditions in the narrowest part is given by:

$$p_{cr} = \left[\frac{2}{\kappa+1}\right]^{\frac{\kappa}{\kappa-1}} \cdot p_{up} \tag{A4}$$

Energy Balance

The internal energy balance of every cylinder is given by the enthalpy flows $\dot{H}_{k,i}$, the heat transfer and the instantaneous work done:

$$\frac{dU_i}{dt} = \dot{H}_{IV,i} + \dot{H}_{CV,i} - \dot{H}_{EV,i} - \dot{Q}_i - p_{cyl,i} \cdot \dot{V}_{cyl,i} \tag{A5}$$

where $\dot{Q}_i$ is the heat transfer to and from the walls. The cylinder volume $V_{cyl,i}$ depends on the cylinder's crank angle position

$$V_{cyl,i}(\phi_i) = V_{cyl,TDC} + A_{cyl} \cdot (l + r \cdot (1 - \cos\phi_i)) - A_{cyl} \cdot \left(\sqrt{l^2 - r^2 \cdot \sin^2\phi_i}\right) \tag{A6}$$

where r is the crank radius, l is the length of the connecting rod and A_{cyl} is the piston area. The cylinder temperatures and pressures are calculated using the definition of the internal energy:

$$\vartheta_{cyl,i} = \frac{U_i}{m_{cyl,i} \cdot c_{v,a}} \tag{A7}$$

and the ideal gas equation:

$$p_{cyl,i} = \frac{m_{cyl,i} \cdot R_a \cdot \vartheta_{cyl,i}}{V_{cyl,i}} \tag{A8}$$

respectively, where $c_{v,a}$ is the specific heat of air at constant volume. The instantaneous torque T_i of each cylinder is defined as:

$$T_i = p_{cyl,i} \cdot A_{cyl} \cdot \left[r \cdot \sin\phi_i + \frac{r^2 \cdot \sin\phi_i \cdot \cos\phi_i}{\sqrt{l^2 - r^2 \cdot \sin^2\phi_i}}\right] \tag{A9}$$

Conservation of Angular Momentum

The law of the conservation of angular momentum determines the engine's acceleration:

$$J_e \cdot \frac{d\omega_e}{dt} = \sum T_i - T_{fric}(\omega_e) + T_{ES}(\omega_e) \tag{A10}$$

where J_e is the engine's inertia and T_{fric} is the friction torque. The engine speed ω_e is the time derivative of any crank angle:

$$\frac{d\phi_i}{dt} = \omega_e \tag{A11}$$

APPENDIX B: CATALYST TEMPERATURE

This section discusses the influence of the pneumatic start on the catalyst temperature which is an important issue for the implementation.

During the pneumatic engine start, the pressurized air from the tank is expanded in the cylinder to produce a torque that accelerates the engine. This expansion decreases the temperature of the gas flowing through the catalyst. The cold gas might lower the catalyst temperature leading to an efficiency drop of the latter.

Due to the lack of a catalytic converter on the test bed no analysis has yet been performed. Here, several qualitative arguments are given on how the temperature of the catalyst is influenced. Firstly, the number of pneumatic power strokes to start the engine is only 2-6 as shown in Figure 14. Hence, the total amount of cold gas leaving the cylinders is very low. Secondly, the cold gas will be heated up by the hot exhaust pipes before it reaches the catalyst. If the cooling of the catalyst remains an issue, the number of pneumatic power strokes can be further reduced by an earlier switch to the combustion mode during the engine start.

APPENDIX C: INFLUENCE OF THE AIR TEMPERATURE IN THE TANK

During the operation of the engine also the air temperature in the tank can vary. However, according to the arguments mentioned in Section 2 the relative variation of the tank temperature is restricted to a significantly smaller range than the relative variation of the tank pressure. Hence, a variation of the tank temperature is not taken into account in the design methodology. To justify this simplification the optimal CV design is computed for various tank temperatures using the PSO algorithm. The results are shown in Figure A2. The two top plots show that the resulting optimal CV timings only vary within a very small range. For all design temperatures, the resulting start time is $t_s = 350$ ms. The bottom plot of Figure A2 shows that the air mass used increases with lower temperature due to the temperature dependence of the air density.

The dashed line shows the air consumption of the design given in Table 4 for various temperatures. This design has a slightly lower air consumption but the start time t_s is 1-4 ms above the limit $t_{s,max} = 350$ ms.

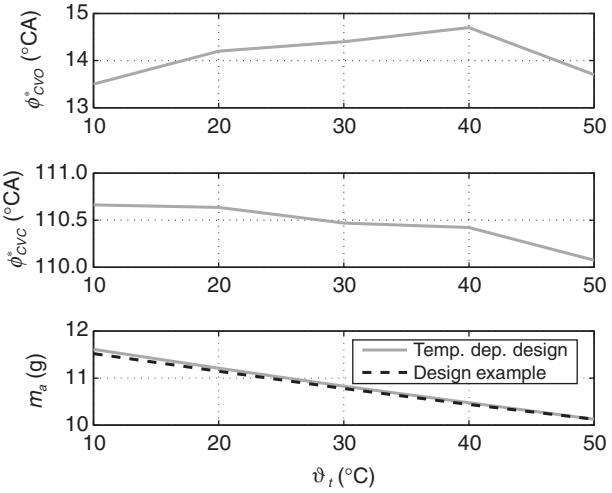

Figure A2

Optimal CV timings and resulting air consumption obtained for CV designs optimized at the respective tank temperature (temp. dep. design). The air consumption obtained with the design given in Table 4 is also shown (design example). This design yields a slightly lower air consumption but exceeds the maximum start time limit $t_{s,max}$ by 1-4 ms at temperatures below 50°C.